

# Non-Darcy Convective Heat and Mass Transfer Flow in a Vertical Channel

Dr. P. Sreenivasa Rao

Department of Physics, Jyothishmathi Institute of Technology & Sciences, Karimnagar, Telengana

## Abstract

We make an attempt to investigate non-Darcy convective heat and Mass transfer flow of a viscous chemically reacting fluid in a vertical channel .The Brinkman Forchheimer extended Darcy equations are used in the governing linear momentum equation, which are solve numerically by using Galerkin finite element technique. The velocity, temperature, concentration, shear stress and rate of Heat and Mass transfer are evaluated numerically for different variations .It is noticed that the temperature and concentration reduce while the velocity increases in the degenerating chemical reaction ( $\gamma > 0$ ) while in the generating case( $\gamma < 0$ ), they reduce in the entire flow region The rate of heat and mass transfer reduce and the skin friction increases on the walls with increase in  $\gamma > 0$ , while a reversed effect is noticed with  $\gamma < 0$ .

**Keywords:** Non-Darcy Flow, Porous Medium, Chemical reaction, Vertical Channel

## 1. INTRODUCTION

The vertical channel is a frequently encountered configuration in thermal engineering equipment, for example, collectors of solar energy, cooling devices of electronic and micro-electronic equipments etc. The influence of electrically conducting the case of fully developed mixed convection between horizontal parallel plates with a linear axial temperature distribution was solved by Gill and Casal (10). Ostrach (16) solved the problem of fully developed mixed convection between vertical plates with and without heat sources. Cebeci et al (6) performed numerical calculations of developing laminar mixed convection between vertical parallel plates for both cases of buoyancy aiding and opposing conditions. Wirtz and McKinley (26) conducted an experimental study of a opposing mixed convection between vertical parallel plates with one plate heated and the other adiabatic. Al-Nimir and Haddad (1) have described the fully developed free convection in an open-ended vertical channel partially filled with porous material. Greif et al (11) have made an analysis on the laminar convection of a radiating gas in a vertical channel. Gupta and Gupta (12) have studied the radiation effect on a hydro magnetic convective flow in a vertical channel. Datta and Jana (8) have studied the effect of wall conductance on a hydro magnetic convection of a radiation gas in a vertical channel. The combined forced and free convective flow in a vertical channel with viscous dissipation and isothermal –isoflux boundary conditions have been studied by Barletta (2). Barletta et al (3) have presented a dual mixed convection flow in a vertical channel. Barletta et al (4) have described a buoyancy MHD flow in a vertical channel.

Non – Darcy effects on natural convection in porous media have received a great deal of attention in recent years because of the experiments conducted with several combinations of solids and fluids covering wide ranges of governing parameters which indicate that the experimental data for systems other than glass water at low Rayleigh numbers, do not agree with theoretical predictions based on the Darcy flow model. This divergence in the heat transfer results has been reviewed in detail in Cheng (7) and Prasad et al. (18) among others. Extensive effects are thus being made to include the inertia and viscous diffusion terms in the flow equations and to examine their effects in order to develop a reasonable accurate mathematical model for convective transport in porous media. The work of Vafai and Tien (24) was one of the early attempts to account for the boundary and inertia effects in the momentum equation for a porous medium. They found that the momentum boundary layer thickness is of order of  $\sqrt{\frac{k}{\varepsilon}}$ . Vafai and Thiyagaraja (25) presented analytical solutions for the velocity and temperature fields for the interface region using the Brinkman Forchheimer –extended Darcy equation. Detailed accounts of the recent efforts on non-Darcy convection have been recently reported in Tien and Hong (21), Cheng (7), and Kalidas and Prasad (13). Here, we will restrict our discussion to the vertical cavity only. Poulikakos and Bejan (19) investigated the inertia effects through the inclusion of Forchheimer velocity squared term, and presented the boundary layer analysis for tall cavities. They also obtained numerical results for a few cases in order to verify the accuracy of their boundary layer analysis for tall cavities. They also obtained numerical results for a few cases in order to verify the accuracy of their boundary layer solutions. Later, Prasad and Tuntomo (17) reported an extensive numerical work for a wide range of parameters, and demonstrated that effects of Prandtl number remain almost unaltered while the dependence on the modified Grashof number,  $Gr$ , changes significantly with an increase in the Forchheimer number. This result in reversal of flow regimes from boundary layer to asymptotic to conduction as the contribution of the inertia term increases in comparison with that of the boundary term. They also reported a criterion for the Darcy flow limit.

The Brinkman – Extended – Darcy modal was considered in Tong and Subramanian (22), and Lauriat and Prasad (15) to examine the boundary effects on free convection in a vertical cavity. While Tong and Subramanian performed a Weber – type boundary layer analysis, Lauriat and Prasad solved the problem numerically for  $A=1$  and  $5$ . It was shown that for a fixed modified Rayleigh number,  $Ra$ , the Nusselt number; decrease with an increase in the Darcy number; the reduction being larger at higher values of  $Ra$ . A scale analysis as well as the computational data also showed that the transport term  $(v \cdot \nabla)v$ , is of low order of magnitude compared to the diffusion plus buoyancy terms. A numerical study based on the Forchheimer-Brinkman-Extended Darcy equation of motion has also been reported recently by Beckerman et al (5). They demonstrated that the inclusion of both the inertia and boundary effects is important for convection in a rectangular packed – sphere cavity. Umadevi et al (23) have studied the chemical reaction effect on Non-Darcy convective heat and mass transfer flow through a porous medium in a vertical channel with heat sources. Deepthi et al (9) and Kamalakar et al (14) have discussed the numerical study of non-Darcy convective heat and mass transfer flow in a vertical channel with constant heat sources under different conditions..

Keeping the above application in view we made an attempt to study chemical reaction effects on non-Darcy convective heat and Mass transfer flow of a viscous fluid in a vertical channel with heat generating sources. The Brinkman Forchheimer extended Darcy equations which take into account the boundary and inertia effects are used in the governing linear Momentum equation. In order to obtain a better insight into this complex problem, we make use of Galerkin finite element analysis with Quadratic Polynomial approximations. The velocity, temperature, concentration, shear stress and rate of Heat and Mass transfer are evaluated numerically for different variations of parameter.

## 2. FORMULATION OF THE PROBLEM

We consider a fully developed laminar convective heat and mass transfer flow of a viscous fluid through a porous medium confined in a vertical channel bounded by flat walls. We choose a Cartesian co-ordinate system  $O(x, y, z)$  with  $x$ - axis in the vertical direction and  $y$ -axis normal to the walls. The walls are taken at  $y= \pm L$ . The walls are maintained at constant temperature and concentration. The temperature gradient in the flow field is sufficient to cause natural convection in the flow field .A constant axial pressure gradient is also imposed so that this resultant flow is a mixed convection flow. The porous medium is assumed to be isotropic and homogeneous with constant porosity and effective thermal diffusivity. The thermo physical properties of porous matrix are also assumed to be constant and Boussinesq approximation is invoked by confining the density variation to the buoyancy term. In the absence of any extraneous force flow is unidirectional along the  $x$ -axis which is assumed to be infinite.

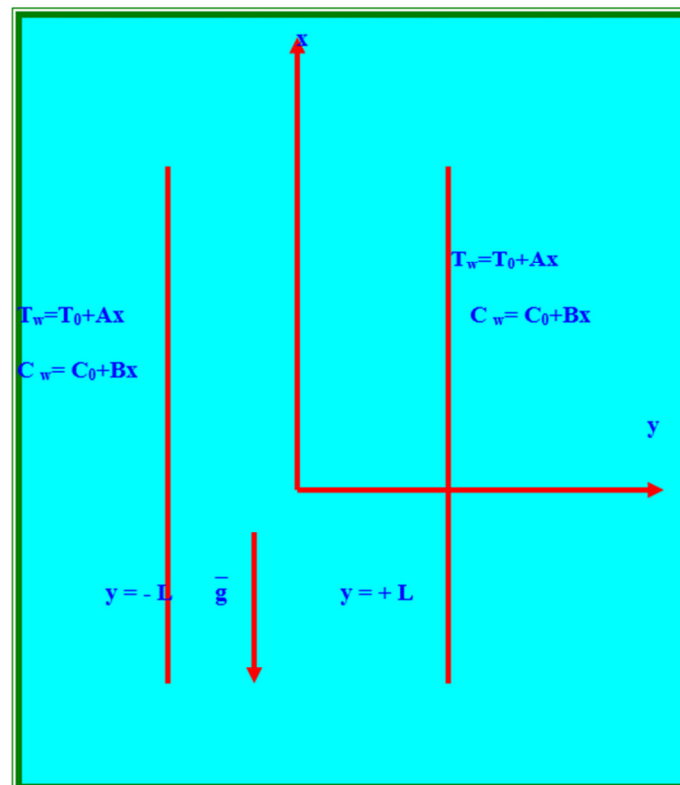


Fig.1 : Configuration of the problem

The momentum, energy and diffusion equations in the scalar form are

$$-\frac{\partial p}{\partial x} + \left(\frac{\mu}{\delta}\right) \frac{\partial^2 u}{\partial y^2} - \left(\frac{\mu}{k}\right)u - \frac{\rho\delta F}{\sqrt{k}}u^2 - \rho g = 0 \quad (1)$$

$$\rho_0 C_p u \frac{\partial T}{\partial x} = k_f \frac{\partial^2 T}{\partial y^2} \quad (2)$$

$$u \frac{\partial C}{\partial x} = D_1 \frac{\partial^2 C}{\partial y^2} - k_1 C \quad (3)$$

The relevant boundary conditions are

$$u = 0, \quad T = T_w, \quad C = C_w \quad \text{at} \quad y = \pm L \quad (4)$$

where  $u$ ,  $T$ ,  $C$  are the velocity, temperature and Concentration,  $p$  is the pressure,  $\rho$  is the density of the fluid,  $C_p$  is the specific heat at constant pressure,  $\mu$  is the coefficient of viscosity,  $k$  is the permeability of the porous medium,  $\delta$  is the porosity of the medium,  $\beta$  is the coefficient of thermal expansion,  $k_f$  is the coefficient of thermal conductivity,  $F$  is a function that depends on the Reynolds number and the microstructure of porous medium,  $\beta^*$  is the volumetric coefficient of expansion with mass fraction concentration,  $k_1$  is the chemical reaction coefficient and  $D_1$  is the chemical molecular diffusivity,  $q_R$  is the radiative heat flux,  $k_{11}$  is the cross diffusivity. Here, the thermo physical properties of the solid and fluid have been assumed to be constant except for the density variation in the body force term (Boussinesq approximation) and the solid particles and the fluids are considered to be in the thermal equilibrium).

Following Tao (20), we assume that the temperature and concentration of the both walls is  $T_w = T_0 + Ax$ ,  $C_w = C_0 + Bx$  where  $A$  and  $B$  are the vertical temperature and concentration gradients which are positive for buoyancy –aided flow and negative for buoyancy –opposed flow, respectively,  $T_0$  and  $C_0$  are the upstream reference wall temperature and concentration respectively. The velocity depend only on the radial coordinate and all the other physical variables except temperature, concentration and pressure are functions of  $y$  and  $x$ ,  $x$  being the vertical co-ordinate

The temperature and concentration inside the fluid can be written as

$$T = T^*(y) + Ax, \quad C = C^*(y) + Bx$$

We define the following non-dimensional variables as

$$u' = \frac{u}{(v/L)}, \quad (x', y') = (x, y)/L, \quad p' = \frac{p\delta}{(\rho v^2/L^2)} \quad (5)$$

$$\theta(y) = \frac{T^* - T_0}{P_1 AL}, \quad C = \frac{C^* - C_0}{P_1 BL}, \quad P_1 = \frac{dp}{dx}$$

Introducing these non-dimensional variables the governing equations in the dimensionless form reduce to (on dropping the dashes)

$$\frac{d^2 u}{dy^2} = 1 + \delta(D^{-1})u - \delta G(\theta + NC) - \delta^2 \Delta u^2 \quad (6)$$

$$\frac{d^2 \theta}{dy^2} = (P_r)u \quad (7)$$

$$\frac{d^2 C}{dy^2} - \gamma C = (Sc)u \quad (8)$$

Where

$$\Delta = FD^{-1/2} \quad (\text{Inertia or Forchheimer parameter}) \quad G = \frac{\beta g AL^3}{v^2} \quad (\text{Grashof Number}) \quad D^{-1} = \frac{L^2}{k} \quad (\text{Inverse$$

$$\text{Darcy parameter}) \quad Sc = \frac{v}{D_1} \quad (\text{Schmidt number})$$

$$N = \frac{\beta^* B}{\beta A} \text{ (Buoyancy ratio)} \quad P_r = \frac{\mu C_p}{k_f} \text{ (Prandtl Number)}$$

$$\gamma = \frac{k_1 L^2}{D_1} \text{ (Chemical reaction parameter)}$$

The corresponding boundary conditions are

$$u = 0, \quad \theta = 0, \quad C = 0 \quad \text{on } y = \pm 1 \quad (9)$$

### 3. FINITE ELEMENT ANALYSIS

To solve these differential equations with the corresponding boundary conditions, we assume if  $u^i, \theta^i, c^i$  are the approximations of  $u, \theta$  and  $C$  we define the errors (residual)  $E_u^i, E_\theta^i, E_c^i$  as

$$E_u^i = \frac{d}{d\eta} \left( \frac{du^i}{d\eta} \right) - D^{-1}u^i + \delta^2 A(u^i)^2 - \delta G(\theta^i + NC^i) \quad (10)$$

$$E_c^i = \frac{d}{dy} \left( \frac{dC^i}{dy} \right) - \gamma C^i - Sc u^i \quad (11)$$

$$E_\theta^i = \frac{d}{dy} \left( \frac{d\theta^i}{dy} \right) - P_r u^i \quad (12)$$

where

$$u^i = \sum_{k=1}^3 u_k \psi_k \quad C^i = \sum_{k=1}^3 C_k \psi_k \quad \theta^i = \sum_{k=1}^3 \theta_k \psi_k \quad (13)$$

These errors are orthogonal to the weight function over the domain of  $e^i$  under Galerkin finite element technique we choose the approximation functions as the weight function. Multiply both sides of the equations (10-12) by the weight function i.e. each of the approximation function  $\psi_j^i$  and integrate over the typical three noded linear element ( $\eta_e, \eta_{e+1}$ ) we obtain

Where

$$\int_{\eta_e}^{\eta_{e+1}} \left( \frac{d}{d\eta} \left( \frac{du^i}{d\eta} \right) - D^{-1}u^i + \delta^2 A(u^i)^2 - \delta G(\theta^i + NC^i) \right) \psi_j^i dy = 0 \quad (14)$$

$$\int_{\eta_e}^{\eta_{e+1}} \left( \frac{d}{dy} \left( \frac{dC^i}{dy} \right) - \gamma C^i - Sc u^i \right) \psi_j^i dy = 0 \quad (15)$$

$$\int_{\eta_e}^{\eta_{e+1}} \left( \frac{d}{dy} \left( \frac{d\theta^i}{dy} \right) - P_r u^i \right) \psi_j^i dy = 0 \quad (16)$$

Choosing different  $\psi_j^i$ 's corresponding to each element  $\eta_e$  in the equation (14)-(16) yields a local stiffness matrix of order  $3 \times 3$  in the form

$$(f_{i,j}^k)(u_i^k) - \delta G(g_{i,j}^k)(\theta_i^k + NC_i^k) + \delta D^{-1}(m_{i,j}^k)(u_i^k) + \delta^2 A(n_{i,j}^k)(u_i^k) = (Q_{i,j}^k) + (Q_{2,j}^k) \quad (17)$$

$$((e_{i,j}^k) - \gamma)(C_i^k) - Sc(m_{i,j}^k)(u_i^k) = R_{1,j}^k + R_{2,j}^k \quad (18)$$

$$((l_{i,j}^k))(\theta_i^k) - P_r(t_{i,j}^k)(u_i^k) = S_{1,j}^k + S_{2,j}^k \quad (19)$$

Where

$(f_{i,j}^k), (g_{i,j}^k), (m_{i,j}^k), (n_{i,j}^k), (e_{i,j}^k), (t_{i,j}^k)$  are  $3 \times 3$  matrices and  $(Q_{2,j}^k), (Q_{1,j}^k), (R_{2,j}^k), (R_{1,j}^k), (S_{2,j}^k)$  and  $(S_{1,j}^k)$  are  $3 \times 1$  column matrices and such stiffness matrices in terms of local nodes in each element are assembled using inter element continuity and equilibrium conditions to obtain the coupled global matrices in terms of the global

nodal values of  $u$ ,  $\theta$  &  $C$  ((17)-(19)). The resulting coupled stiffness matrices are solved by iteration process. This procedure is repeated till the consecutive values of  $u_i$ 's,  $\theta_i$ 's and  $C_i$ 's differ by a preassigned percentage

#### 4. SHEAR STRESS, NUSSULT NUMBER AND SHERWOOD NUMBER

The shear stress on the boundaries  $y = \pm 1$  is given by

$$\tau_{y=\pm L} = \mu \left( \frac{du}{dy} \right)_{y=\pm L}$$

In the non-dimensional form is

$$\tau_{y=\pm 1} = \left( \frac{du}{dy} \right)_{y=\pm 1}$$

The rate of heat transfer (Nusselt Number) is given by

$$Nu_{y=\pm i} = \left( \frac{d\theta}{dy} \right)_{y=\pm 1}$$

The rate of mass transfer (Sherwood Number) is given by

$$Sh_{y=\pm 1} = \left( \frac{dC}{dy} \right)_{y=\pm 1}$$

#### 5. DISCUSSION OF THE NUMERICAL RESULTS

In order to get physical insight into the problem we have carried out numerical calculations for non-dimensional velocity, temperature and species concentration, skin-friction, Nusselt number and Sherwood number by assigning some specific values to the parameters entering into the problem.

##### Effects of parameters on velocity profiles:

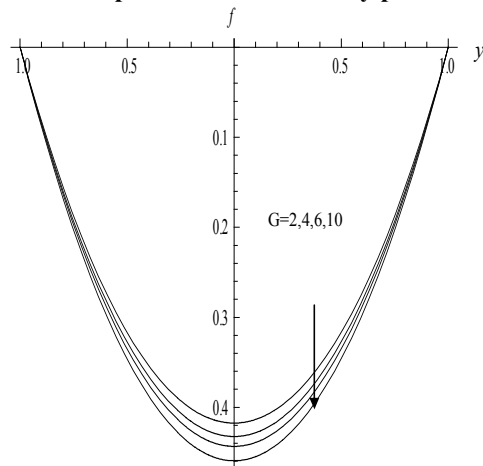


Fig. 2a: Variation of  $u$  with  $G$   
 $D^{-1}=0.2$ ,  $Sc=1.3$ ,  $N=1$ ,  $Pr=0.71$ ,  
 $\gamma=0.5$

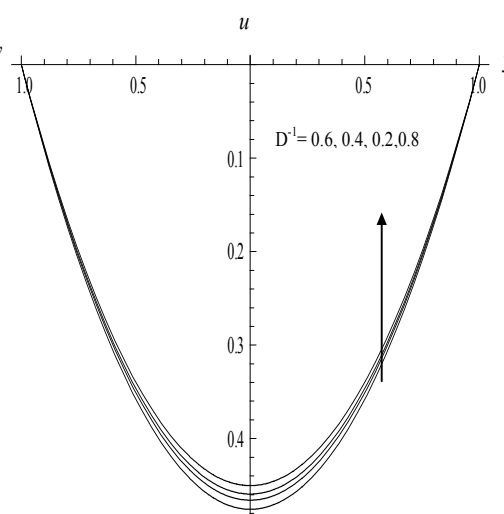


Fig. 3a: Variation of  $u$  with  $D^{-1}$   
 $G=2$ ,  $Sc=1.3$ ,  $N=1$ ,  $Pr=0.71$ ,  $\gamma=0.5$

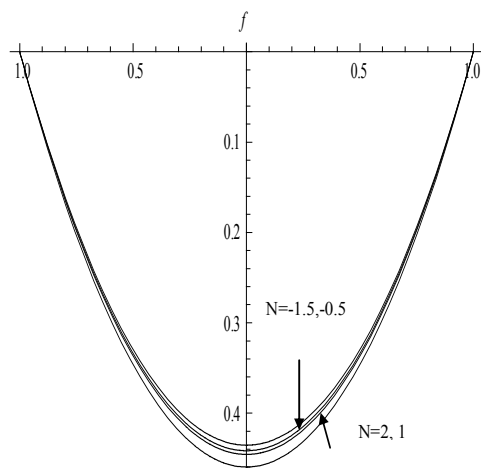


Fig. 4a Variation of  $u$  with  $N$   
 $G=2, D^{-1}=0.2, Sc=1.3, Pr=0.71, \gamma=0.5$

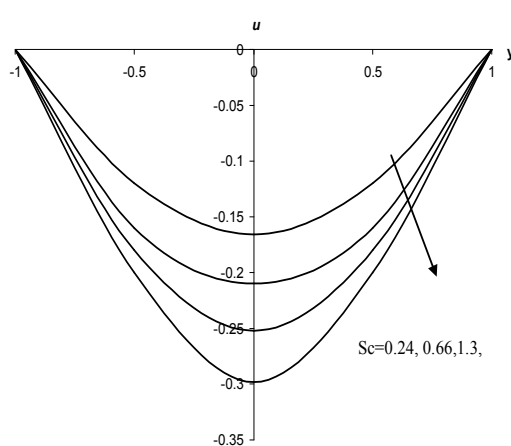


Fig. 5a: Variation of  $u$  with  $Sc$   
 $G=2, D^{-1}=0.2, N=1, Pr=0.71, \gamma=0.5$

Fig.2a shows the variation of the velocity with Grashof number  $G$  at any point in the flow region. It decreases with increase in the buoyancy parameter ( $G$ ). The maximum of  $u$  occurs at  $y=0.0$ . Fig.3a represents the  $u$  with the inverse Darcy parameter ( $D^{-1}$ ). The axial velocity reduces with increase in  $D^{-1} \leq 0.6$  and increases with further higher  $D^{-1} \geq 0.8$ . This is due to the fact that when the magnetic field is applied normal to the boundaries; ponder motive force acts in the upward direction to decrease the fluid velocity. Also the presence of the porous medium enhances the resistance to the flow resulting in the reduction of the velocity field.

Fig.4a exhibits the variation of  $u$  with buoyancy ratio ( $N$ ). It is found that when the molecular buoyancy force dominates over the thermal buoyancy force the axial velocity decreases when the buoyancy forces are in the same direction and for the forces are in opposite directions, it increases in the flow region. Fig.5a shows the variation of  $u$  with Schmidt number ( $Sc$ ). It is found that the velocity enhances with increases in  $Sc$ . This is due to the fact that increasing  $Sc$  means reducing molecular diffusivity, therefore lesser the molecular diffusivity larger the velocity in the fluid region.

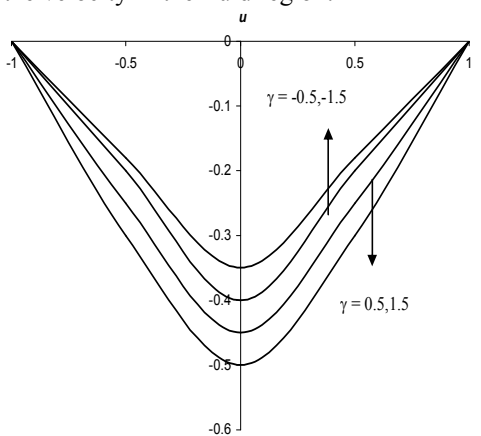


Fig. 6a: Variation of  $u$  with  $\gamma$   
 $G=2, D^{-1}=0.2, Sc=1.3, N=1, Pr=0.71$

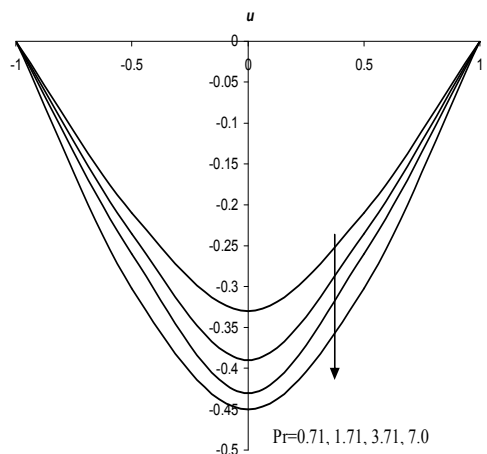


Fig.7a: Variation of  $u$  with  $Pr$   
 $G=2, D^{-1}=0.2, Sc=1.3, N=1, \gamma=0.5$

The effect of chemical reaction parameter ( $\gamma$ ) on  $u$  is exhibited in fig.6a. It is found that the axial velocity enhances with increase in  $\gamma$  in the entire flow region in the degenerating chemical reaction case while in the generating chemical reaction case the velocity reduces in the flow region. Fig.7a represents the variation of  $u$  with Prandtl number ( $Pr$ ). An increase in  $Pr$  increases the velocity in the flow region. This is due to the fact that increasing  $Pr$  increases the thickness of the momentum boundary layer which in turn increases the velocity in the flow region.

#### Effects of parameters on temperature profiles:

The non-dimensional temperature ( $\theta$ ) is shown in figs.2b-8b for different parametric representation. We follow the convention that the non-dimensional temperature ( $\theta$ ) is positive/negative according as the actual

temperature ( $T^*$ ) is greater/lesser than the reference temperature  $T_0$ . Fig.2b exhibits the temperature with  $G$ . It is found that the actual temperature reduces with increase in Grashof number with maximum attained at  $y=0$ . With reference to  $D^{-1}$  we find that the actual temperature decreases with increasing values of  $D^{-1} \leq 0.6$  and enhances with  $D^{-1} \geq 0.8$ . This is due to the fact that the thickness of the boundary layer decreases owing to the Darcy drag developed by the porous medium (Fig.3b). Fig.4b shows the variation of  $\theta$  with buoyancy ratio ( $N$ ). It is observed from the profiles that when the molecular buoyancy force dominates over the thermal buoyancy force the actual temperature reduces when the buoyancy forces are in the same direction and for the forces are in opposite directions it increases in the flow region. Fig.5b represents  $\theta$  with  $Sc$ . It is found that lesser the molecular diffusivity lesser the actual temperature in the entire flow region. Fig.6b represents  $\theta$  with chemical reaction parameter ( $\gamma$ ). From the profiles we find that the actual temperature reduces with increase in  $\gamma$  in both the degenerating /generating chemical reaction cases. Fig.7b shows the variation of  $\theta$  with Prandtl number ( $Pr$ ). As the Prandtl number increases there is a significant reduction in the thermal boundary layer with a fall in the actual temperature throughout the flow region, since enhancement of  $Pr$  amounts to reduction of thermal diffusion.

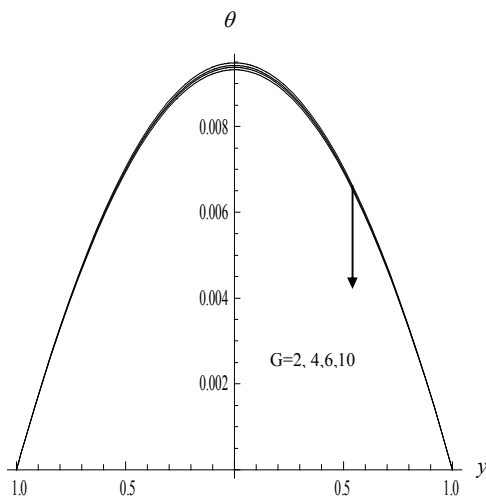


Fig. 2b: Variation of  $\theta$  with  $G$   
 $D^{-1}=0.2, Sc=1.3, N=1, Pr=0.71, \gamma=0.5$

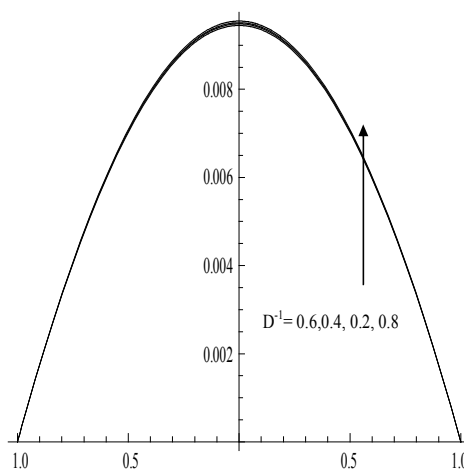


Fig. 3b Variation of  $\theta$  with  $D^{-1}$   
 $G=2, Sc=1.3, N=1, Pr=0.71, \gamma=0.5$

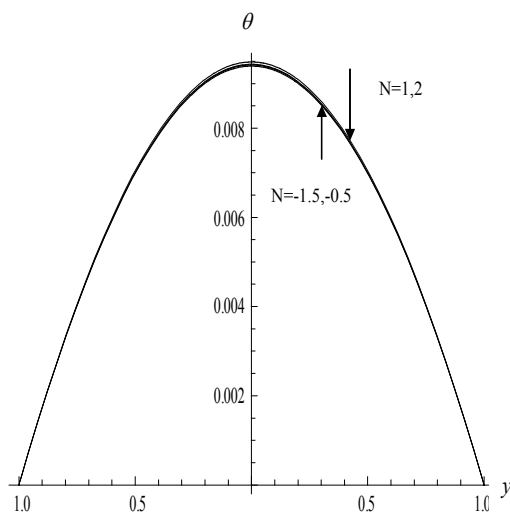


Fig. 4b Variation of  $\theta$  with  $N$   
 $G=2, D^{-1}=0.2, Sc=1.3, Pr=0.71, \gamma=0.5$

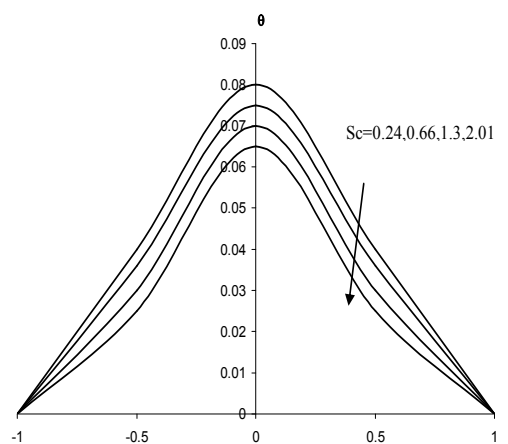


Fig. 5b: Variation of  $\theta$  with  $Sc$   
 $G=2, D^{-1}=0.2, N=1, Pr=0.71, \gamma=0.5$

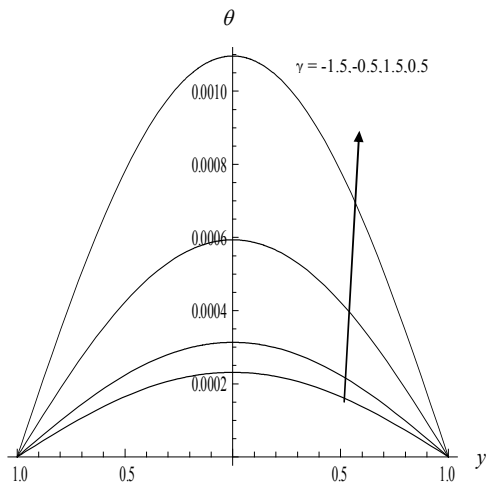


Fig. 6b: Variation of  $\theta$  with  $\gamma$   
 $G=2, D^{-1}=0.2, Sc=1.3, N=1, Pr=0.71$

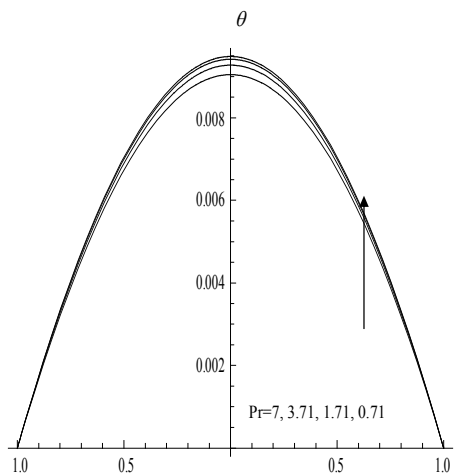


Fig. 7b: Variation of  $\theta$  with  $Pr$   
 $G=2, D^{-1}=0.2, Sc=1.3, N=1, \gamma=0.5$

**Effects of parameters on concentration profiles:**

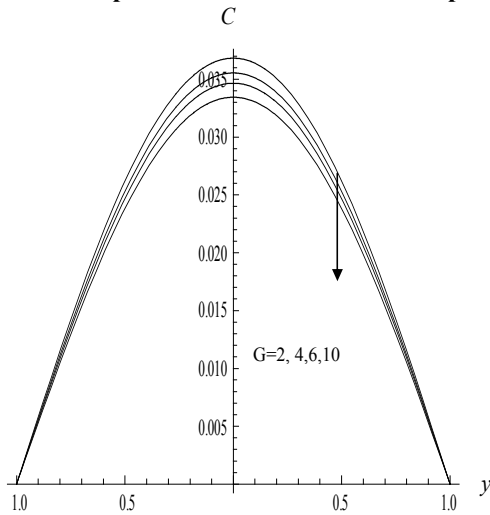


Fig. 2c: Variation of  $C$  with  $G$   
 $D^{-1}=0.2, Sc=1.3, N=1, Pr=0.71, \gamma=0.5$

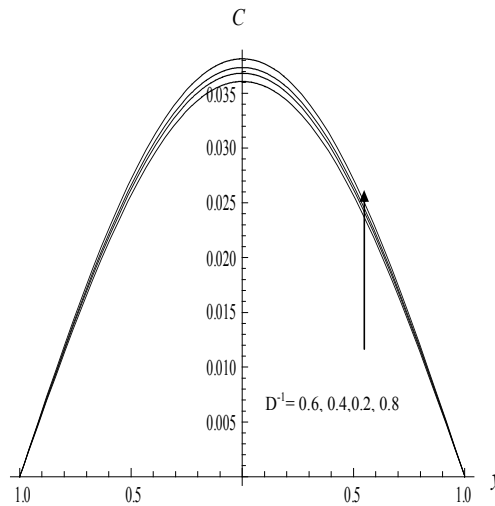


Fig. 3c: Variation of  $c$  with  $D^{-1}$   
 $G=2, Sc=1.3, N=1, Pr=0.71, \gamma=0.5$

The non-dimensional concentration ( $C$ ) is shown in figs.2c-8c for different parametric variations. We follow the convention that the non-dimensional concentration ( $C$ ) is positive/negative according as the actual concentration ( $C^*$ ) is greater/lesser than the reference concentration ( $C_o$ ). Fig.2c shows the variation of Concentration with Grashof number  $G$ . It can be seen from the profiles that the actual concentration reduces with increasing  $G$ . Fig.3c represents  $C$  with  $D^{-1}$ . We find that lesser the permeability of the porous medium ( $D^{-1} \leq 0.6$ ) smaller the actual concentration and for further lowering of the permeability larger the actual concentration in the entire flow region.



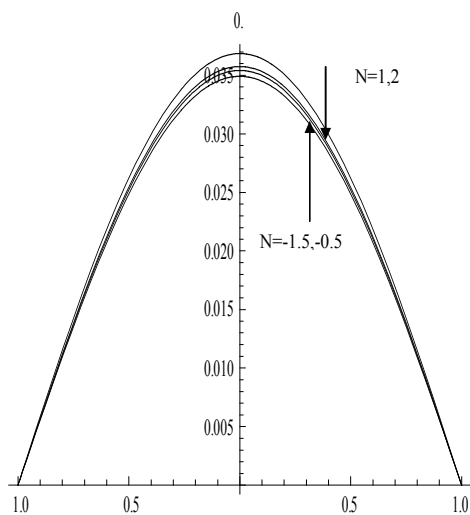


Fig. 4c Variation of C with N  
 $G=2, D^{-1}=0.2, Sc=1.3, Pr=0.71, \gamma=0.5$

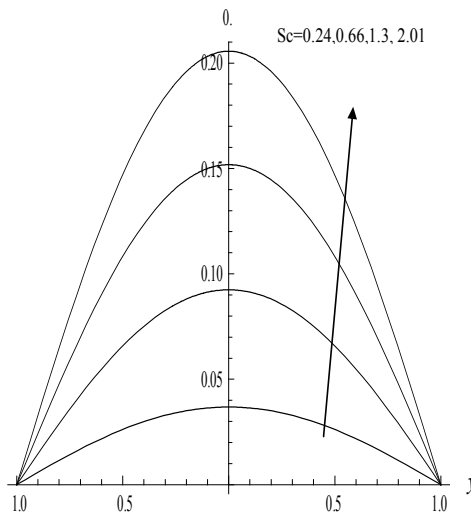


Fig. 5c: Variation of C with Sc  
 $G=2, D^{-1}=0.2, N=1, Pr=0.71, \gamma=0.5,$

Fig.4c shows the variation of C with buoyancy ratio N. We find that when the molecular buoyancy force dominates over the thermal buoyancy force the actual concentration increases in the flow region irrespective of the directions of the buoyancy forces. Fig.5c shows the variation of C with Sc. It can be seen from the profiles that the actual concentration enhances with increase in Sc.

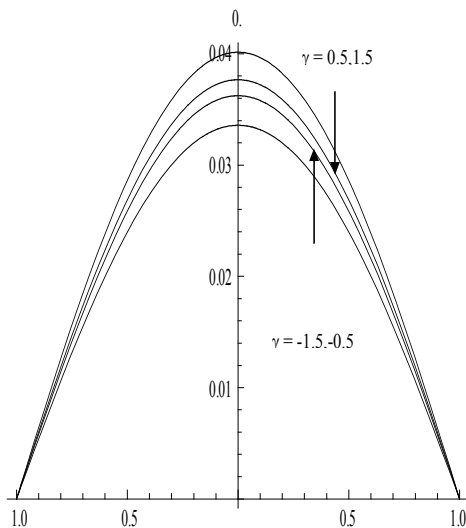


Fig.6c: Variation of C with  $\gamma$   
 $G=2, D^{-1}=0.2, Sc=1.3, N=1, Pr=0.71$

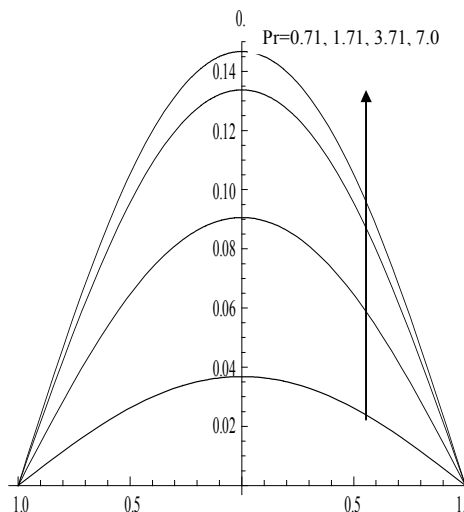


Fig. 7c: Variation of C with Pr  
 $G=2, D^{-1}=0.2, Sc=1.3, N=1, \gamma=0.5$

Fig.6c shows the variation of C with Chemical reaction parameter ( $\gamma$ ). It can be seen from the profiles that the actual concentration reduces in both the degenerating /generating chemical reaction cases in the entire flow region. Fig. 7c. exhibits the variation of C with Prandtl number (Pr).As the Prandtl number increases there is a marginal increase in the actual concentration. This is due to the fact the enhancement of Prandtl number amounts to reduction of thermal diffusion.

**Effects of parameters on Skin friction, Nusselt number and Sherwood number:**

The Skin friction, the rate of heat and mass transfer at the boundaries  $y=\pm 1$  is exhibited in table.1.

Table -1

	$\tau(1)$	$\tau(-1)$	Nu(1)	Nu(-1)	Sh(1)	Sh(-1)	
G	2	0.905897	-0.905897	0.0151438	-0.0151438	0.0495079	-0.0495079
	4	0.879052	-0.879052	0.0149699	-0.0149699	0.0399606	-0.0399606
	6	0.867768	-0.867768	0.0139654	-0.0139654	0.0368572	-0.0368572
	10	0.845212	-0.845212	0.0129551	-0.0129551	0.0336514	-0.0336514
$D^{-1}$	0.2	0.905897	-0.905897	0.0151438	-0.0151438	0.0495079	-0.0495079
	0.4	0.912073	-0.912073	0.0159694	-0.0159694	0.0500453	-0.0500453
	0.6	0.914682	-0.914682	0.0162117	-0.0162117	0.0511453	-0.0511453
	0.8	0.917703	-0.917703	0.0165318	-0.0165018	0.0523351	-0.0523351
N	1.0	0.905897	-0.905897	0.0182438	-0.0182438	0.0495379	-0.0495079
	2.0	0.898419	-0.898419	0.0181713	-0.0181713	0.0449901	-0.0449901
	-0.5	0.911432	-0.911432	0.0181152	-0.0181152	0.0480718	-0.0480771
	-1.5	0.919737	-0.919737	0.0181098	-0.0181098	0.0491045	-0.0491045
Pr	0.71	0.905897	-0.905897	0.0182467	-0.0182467	0.0495379	-0.0495379
	1.71	0.919835	-0.919835	0.0196092	-0.0196092	0.0474431	-0.0474431
	3.71	0.919834	-0.91983	0.0200284	-0.0200284	0.0452547	-0.0452547
	7.0	0.919822	-0.919822	0.0285406	-0.0285406	0.0439482	-0.0439482
$\gamma$	0.5	0.905897	-0.905897	-0.0182467	-0.314769	0.0609886	-0.0609886
	1.5	0.91984	-0.91984	-0.0181722	-0.307166	0.0547955	-0.0547955
	-0.5	0.919767	-0.919767	-0.0181751	-0.307136	0.0649491	-0.0649491
	-1.5	0.91972	-0.91972	-0.018177	-0.307116	0.0715908	-0.0715908
Sc	0.24	0.934437	-0.936837	0.0182438	-0.0182438	0.0585079	-0.0585079
	0.66	0.918782	-0.918782	0.0181682	-0.0181982	0.147383	-0.147383
	1.3	0.916794	-0.916794	0.0182015	-0.0182215	0.230513	-0.230513
	2.01	0.915889	-0.915889	0.0182293	-0.0182493	0.330226	-0.330226

From the tabular values we find that an increase in G or Sc reduces the skin friction on both the wall  $y = \pm 1$ . Lesser the permeability of the porous medium the skin friction increases on the both the walls. When the molecular buoyancy force dominates over the thermal buoyancy force the skin friction reduces on the walls when the buoyancy forces are in the same direction and for the forces acting in opposite directions it increases on the walls. With reference to the chemical reaction parameter ( $\gamma$ ) we find that the skin friction enhances on both the walls in the degenerating chemical reaction case and in the generating chemical reaction case it reduces on the walls. As the Prandtl number increases ( $Pr \leq 1.71$ ) the skin friction enhances on  $y = \pm 1$  and reduces for higher  $Pr \geq 3.71$  on both the walls. The rate of heat transfer (Nusselt number) reduces with increase in G and enhances with  $D^{-1}$  or Pr. It reduces on the walls with increasing in the buoyancy ratio (N) irrespective of the directions of the buoyancy forces. The variation of Nu with Sc shows that lesser the molecular diffusivity ( $Sc \leq 0.66$ ) smaller Nu on  $y = \pm 1$  while for further lowering of the molecular diffusivity ( $Sc \geq 1.3$ ) larger the skin friction on the walls. The magnitude of Nu reduces on  $y = \pm 1$ , with increase in the strength of the heat generating/ absorption source. With respect to the chemical reaction parameter ( $\gamma$ ) we find that the magnitude of Nu reduces in the degenerating chemical reaction case and enhances in the generating chemical reaction case on both the walls. The rate of mass transfer (Sherwood number) reduces with increase G or Pr and enhances with  $D^{-1}$  or Sc on both the walls. With respect to the chemical reaction parameter ( $\gamma$ ) we find that the rate of mass transfer reduces on  $y = \pm 1$  in degenerating chemical reaction case while in the generating case it increases on the walls. The rate of mass transfer reduces with increase in  $N > 0$  and enhances with  $N < 0$  on both the walls.

## 6. CONCLUSIONS:

The non-linear coupled equations governing the flow, heat and mass transfer have been solved by employing Galerkin finite element technique. The velocity, temperature, concentration, skin friction and the rate of heat and mass transfer on the walls have been discussed for different variations of the parameters. The important conclusions of the analysis are:

- 1) An increase in the buoyancy parameter (G) reduces the velocity, temperature and concentration. The skin friction, the rate of heat and mass transfer on reduces on the walls.
- 2) Lesser the permeability of the porous medium smaller the velocity, concentration, temperature and larger the skin friction rate of heat and mass transfer on the walls.
- 3) The velocity, temperature and concentration reduces with increase in the buoyancy ratio ( $N > 0$ ) while for  $N < 0$ , the velocity and temperature increases, the concentration reduces in the flow region. The skin friction, Nusselt number and Sherwood number reduces on the walls with  $N > 0$  and for  $N < 0$ , the skin friction and Sherwood number enhances while the Nusselt number reduces on the walls.

- 4) Lesser the molecular diffusivity smaller the velocity and concentration and smaller the temperature. The skin friction and Nusselt Number reduces and the Sherwood number increases with  $Sc$ .
- 5) The temperature and concentration reduce while the velocity increases with  $\gamma > 0$  while for  $\gamma < 0$ , they reduce in the entire flow region. The rate of heat and mass transfer reduce and the skin friction increases on the walls with increase in  $\gamma > 0$  while a reversed effect is noticed with  $\gamma < 0$ .
- 6) The velocity, temperature and concentration reduce with increase in  $N > 0$  while for  $N < 0$ , we notice an enhancement in the velocity, temperature, reduction in the concentration. The skin friction rate of heat and mass transfer reduce on the walls with increase in  $N > 0$  while for  $N < 0$ , we find an enhancement in skin friction and Sherwood number, reduction in Nusselt Number on the walls.

## 7. REFERENCES

1. Al-Nimir, M.A., Haddad, O.H.: Fully developed free convection in open-ended vertical channels partially filled with porous material, *J. Porous Media*, V.2, pp.179-189 (1999).
2. Barletta, A.: Analysis of combined forced and free flow in a vertical channel with viscous dissipation and isothermal-isoflux boundary conditions, *ASME J. Heat Transfer*, V.121, pp.349-356 (1999).
3. Barletta, A., Magyari, E. and Kellaer, B.: Dual mixed convection flows in a vertical channel, *INny. J. Heat and Mass Transfer*, V.48, pp.4835-4845 (2005).
4. Barletta, A., Celli, M. and Magyari, E. and Zanchini, E.: Buoyancy MHD flows in a vertical channel: the levitation regime, *Heat and Mass Transfer*, V.44, pp.1005-1013 (2007).
5. Beckermann, C., Visakanta, R. and Ramadhyani, S.: A numerical study of non-Darcian natural convection in a vertical enclosure filled with a porous medium, *Numerical Heat Transfer* 10, pp.557-570, (1986).
6. Cebeci, T., Khattab, A.A. and LaMont, R.: Combined natural and forced convection in a vertical ducts, in: *Proc. 7<sup>th</sup> Int. Heat Transfer Conf.*, V.3, pp.419-424 (1982).
7. Cheng: Heat transfer in geothermal systems. *Adv. Heat transfer* 14, 1-105 (1978).
8. Datta, N. and Jana, R.N.: Effect of wall conductance on hydromagnetic convection of a radiation gas in a vertical channel, *Int. J. Heat Mass Transfer*, V.19, pp.1015-1019 (1974).
9. Deepti, J., Prasada Rao, D.R.V.: Finite element analysis of chemically reaction effect on Non-Darcy convective heat and mass transfer flow through a porous medium in a vertical channel with constant heat sources, *Int. J. Math. Arch*, V.3(11), pp.3885-3897 (2012).
10. Gill, W.N. and Del Casal, A.: A theoretical investigation of natural convection effects in a forced horizontal flows, *AIChE J*, V.8, pp.513-518 (1962).
11. Greif, R., Habib, I.S. and Lin, J.C.: Laminar convection of a radiating gas in a vertical channel, *J. Fluid. Mech.*, V.46, p.513 (1971).
12. Gupta, P.S. and Gupta, A.S.: Radiation effect on hydromagnetic convection in a vertical channel, *Int. J. Heat Mass Transfer*, V.127, pp.1437-1442 (1973).
13. Kalidas, N. and Prasad, V.: Benard convection in porous media Effects of Darcy and Prandtl Numbers, *Int. Syms. Convection in porous media, non-Darcy effects*, proc. 25<sup>th</sup> Nat. Heat Transfer Conf. V.1, pp.593-604 (1988).
14. Kamalakar, P.V.S., Prasada Rao, D.R.V. and Raghavendra Rao, R.: Finite element analysis of chemical reaction effect on Non-Darcy convective heat and mass transfer flow through a porous medium in a vertical channel with heat sources, *Int. J. Appl. Math and Mech*, V.8(13), pp.13-28 (2012).
15. Laurait, G. and Prasad, V.: Natural convection in a vertical porous cavity a numerical study of Brinkman extended Darcy formulation, *J. Heat Transfer*, pp.295-320 (1987).
16. Ostrach, S.: Combined natural and forced convection laminar flow and heat transfer of fluid with and without heat sources in channels with linearly varying wall temperature, *NACA TN*, 3141, (1954).
17. Prasad, V. and Tuntomo, A.: Inertia Effects on Natural Convection in a vertical porous cavity, *numerical Heat Transfer*, V.11, pp.295-320 (1987).
18. Prasad, V., F.A., Kulacki and M. Keyhani: "Natural convection in a porous medium" *J. Fluid Mech.* 150p.89-119 (1985).
19. Poulidakos, D., and Bejan, A.: The Departure from Darcy flow in Nat. Convection in a vertical porous layer, *physics fluids* V.28, pp.3477-3484 (1985).
20. Tao, L.N.: On combined and forced convection in channels, *ASME J. Heat Transfer*, V.82, pp.233-238 (1960).
21. Tien, D., and Hong, J.T.: Natural convection in porous media under non-Darcian and non-uniform permeability conditions, hemisphere, Washington, C. (1985).
22. Tong, T.L. and Subramanian, E.: A boundary layer analysis for natural convection in porous enclosures: use of the Brinkman-extended Darcy model, *Int. J. Heat Mass Transfer*, 28, pp.563-571 (1985).
23. Umadevi, B., Sreenivas, G., Bhuvana vijaya, R. and prasada Rao, D.R.V.: Finite element analysis of chemical reaction effect on Non-Darcy mixed convective double diffusive heat transfer flow through a

- porous medium in a vertical channel with constant heat sources., *Adv. Appl. Sci. Res.* V.3 (5), pp.2924-2939(2012).
24. Vafai, K., Tien, C.L: Boundary and Inertia effects on flow and Heat Transfer in Porous Media, *Int. J. Heat Mass Transfer*, V.24. Pp.195-203 (1981).
  25. Vafai, K., Thyagaraju, R.: Analysis of flow and heat Transfer at the interface region of a porous medium, *Int. J. Heat Mass Trans.*, V.30pp.1391-1405 (1987).
  26. Wirtz,R.A and McKinley,P: Buoyancy effects on downward laminar convection between parallel plates.Fundamental of forced and mixed convection,ASME HTD,V.42,pp.105-112(1985).